Room-temperature structural ordering of a Heusler compound Fe$_3$Si

S. Yamada,[1] J. Sagar,[2] S. Honda,[3,4] L. Lari,[2,5] G. Takemoto,[1] H. Itoh,[3,4] A. Hirohata,[6,7] K. Mibu,[8]
M. Miyao,[1,4] and K. Hamaya[1,*]

[1]*Department of Electronics, Kyushu University, 744 Motooka, Fukuoka 819-0395, Japan*
[2]*Department of Physics, The University of York, York YO10 5DD, United Kingdom*
[3]*Department of Pure and Applied Physics, Kansai University, Suita 564-8680, Japan*
[4]*CREST, Japan Science and Technology Agency, Sanbancho, Tokyo 102-0075, Japan*
[5]*The York JEOL Nanocentre, The University of York, York YO10 5BR, United Kingdom*
[6]*Department of Electronics, The University of York, York YO10 5DD, United Kingdom*
[7]*PRESTO, Japan Science And Technology Agency, Kawaguchi, 332-0012, Japan*
[8]*Nagoya Institute of Technology, Nagoya, Aichi 466-8555, Japan*

$D0_3$-ordered Fe$_3$Si, which is one of the ferromagnetic Heusler compounds, has so far been formed by high-temperature heat treatments. Here, we demonstrate room-temperature $D0_3$ ordering of Fe$_3$Si films grown on Ge(111) by using a molecular beam epitaxy (MBE) technique. In our MBE conditions, higher growth temperatures are not effective to obtain highly ordered $D0_3$ structures because of the interfacial reactions between Fe$_3$Si and Ge. Even for the room-temperature growth, the degree of the $D0_3$ ordering can be improved with increasing film thickness. Considering the experimental data and the calculated results based on molecular dynamics, we can understand that the main structural disorder is derived from a specific Fe site in the Fe$_3$Si film near the interface. We also discuss the room-temperature $D0_3$ ordering in terms of the local stoichiometry of the supplied atoms in MBE conditions.

I. INTRODUCTION

Ferromagnetic Heusler compounds, i.e., X_2YZ (X,Y: transition metals, Z: main group element) have been attracting attention for future application in spintronic devices as ferromagnetic electrodes.[1–7] In particular, one of the ferromagnetic Heusler compounds, Fe$_3$Si, has been explored over a long period.[8–19] Since $D0_3$-type Fe$_3$Si has two nonequivalent Fe sites, it has been often referred to as one of the binary Heusler compounds. The bulk Fe$_3$Si with a $D0_3$-ordered structure has a high Curie temperature of ∼800 K.[11] In general, to obtain highly $D0_3$-ordered structure, the formation processes with high temperatures ranging from 700 °C to 1200 °C have so far been required.[8–11,17–19]

However, the Fe$_3$Si films with ordered structures such as $B2$ and $D0_3$ were recently obtained with low-temperature growth below 200 °C.[20–27] Because of the small lattice mismatch between Fe$_3$Si and the semiconductors, the Fe$_3$Si films can be epitaxially grown on semiconductors such as GaAs,[20–22] Si,[23–25] and Ge.[26,27] In particular, we individually established the growth technique for high-quality Fe$_3$Si epitaxial films on Si(111) (Ref. 25) or Ge(111) (Refs. 26 and 27) by means of molecular beam epitaxy (MBE) at 130 °C. The spin polarization of a thin-film sample was experimentally estimated to be ∼0.45 at 4 K (Ref. 22) and ∼0.20 at room temperature,[7] and the electrical detection of spin-polarized electrons in Si and Ge using the Fe$_3$Si electrodes was also achieved.[28,29]

Recently, the local structural ordering of the epitaxial Fe$_{3+x}$Si$_{1−x}$ films was roughly estimated by using conversion electron Mössbauer spectroscopy (CEMS).[27,30,31] Since we obtained atomically flat heterointerfaces between Fe$_3$Si and Ge, a relatively high degree of $D0_3$ ordering, ∼70%, was obtained for stoichiometric samples ($x \sim 0$) even for the

low-temperature growth at 130 °C.[27] Also, the post annealing, generally effective to enhance a degree of crystal ordering,[17–19] could not improve the degree of the $D0_3$ ordering for the stoichiometric samples.

Up to now, Yoshitake *et al.* reported room-temperature epitaxial growth of Fe$_3$Si films on Si(111) by using facing target dc sputtering,[23] but they could not obtain the $D0_3$-ordered Fe$_3$Si. From the viewpoint of high-performance spintronic applications, the fabrication of $D0_3$-ordered Fe$_3$Si is required. In this article, we show an experimental demonstration of the room-temperature (RT) $D0_3$ ordering of the Fe$_3$Si films on Ge(111) by using an MBE technique with Fe and Si Knudsen cells. This paper presents the following contents. First, by using structural analyses, we experimentally show evidence for the presence of $D0_3$-ordered structure in the RT-grown Fe$_3$Si film. Next, we examine the effect of growth temperature on the degree of the $D0_3$ ordering. As a result, the higher growth temperatures are not effective to obtain the highly ordered $D0_3$ structures because of the influence of the interfacial reactions between Fe$_3$Si and Ge. Interestingly, we can find an improvement of the degree of the $D0_3$ ordering with increasing film thickness even for the RT growth. Comparing experimental data with the calculated results based on molecular dynamics, we can understand that the main structural disorder is derived from a specific Fe site in the Fe$_3$Si film near the interface. Finally, we also discuss the thermal stability of the ordered structures in Fe$_3$Si for considering the origin of RT $D0_3$ ordering by our MBE conditions.

II. GROWTH AND CHARACTERIZATIONS

Fe$_3$Si thin films with various thicknesses were directly grown on Ge(111) at various growth temperatures (T_G) of

RT, 130 °C, 250 °C, 300 °C, 350 °C, and 400 °C by low-temperature MBE, where we coevaporated Fe and Si using Knudsen cells.[26,27] Prior to the growth of the Fe_3Si films, Ge(111) substrates were chemically cleaned to remove native oxide and contamination from the surface. The cleaned substrates were loaded into an MBE chamber with a base pressure of $\sim 1 \times 10^{-9}$ Torr. After heat treatment at 550 °C for 20 min, the substrate temperature was reduced down to each T_G. The T_G value was measured with a thermocouple mounted behind a substrate holder. Thus, $T_G =$ RT (~ 25 °C) can be guaranteed during the growth. Also, we performed *in situ* reflection high-energy electron diffraction (RHEED) observations for all the samples during the growth. For $T_G \leqslant$ 300 °C, the RHEED patterns exhibited symmetrical streaks, indicating two-dimensional epitaxial growth of the Fe_3Si films on Ge(111) below 300 °C. For $T_G > 300$ °C, on the other hand, the RHEED patterns became slightly spotty. The crystal structures were characterized by cross-sectional transmission electron microscopy (TEM), nanobeam diffraction (NBD), and high-angle annular dark field (HAADF) imaging. We confirmed the chemical composition of the Fe_3Si layers for any positions by nanobeam energy dispersive x-ray spectroscopy (EDS) (beam size: ~ 1 nmϕ). Magnetic properties and ^{57}Fe Mössbauer spectra were measured with a vibrating sample magnetometer (VSM) and conversion electron Mössbauer spectroscopy (CEMS), respectively, at room temperature. To enhance the detectability in the CEMS measurements, we enriched ^{57}Fe nuclei to 20% in the Knudsen cell of the Fe source.

III. EFFECT OF GROWTH TEMPERATURE

First, we show cross-sectional TEM observations of the Fe_3Si(25 nm)/Ge(111) structures grown at $T_G =$ RT. In Fig. 1(a), we can clearly see the lattice images in the Fe_3Si layer and the atomic-scale abruptness at Fe_3Si/Ge(111) interfaces, which are the same as our previous works.[26,27] We can find atomic steps at the interface (see yellow arrow). By using HAADF imaging techniques, we can also examine the atomic ordering in the Fe_3Si layer along the [1$\bar{1}$0] zone axis. Figure 1(b) shows the intensity profile of the contrast from the areas I and II, enclosed in Fig. 1(a). Since the image intensity is roughly proportional to the square of the atomic number, we can identify the difference in the position between Fe and Si. Surprisingly, the atomic rows with -Si-Fe-Fe-Fe-Si- can be observed from the profile I (left), indicating the presence of the $D0_3$ ordering. It should be noted that the $D0_3$ ordering can be observed from near the top of Ge. From the profile II (right), some disordered rows can also be observed near the atomic steps at the interface. These features imply that even at $T_G =$ RT the $D0_3$ ordering can occur at the early stage of the growth of the Fe_3Si film if the atomic steps of the Ge(111) surface do not affect the interfacial atomic ordering. In the same sample, we also obtained a HAADF image and its intensity profile inside the Fe_3Si layer, as shown in Figs. 1(c) and 1(d), respectively. We can identify the clear atomic rows with . . . -Fe-Si-Fe-Fe-Fe-Si- . . ., which implies the ideal site occupation of each atom with . . . -C-D-A-B-C-D- . . . in the ideal $D0_3$-ordered Fe_3Si along (111), as illustrated in the inset of Fig. 2. This is a direct observation of the site
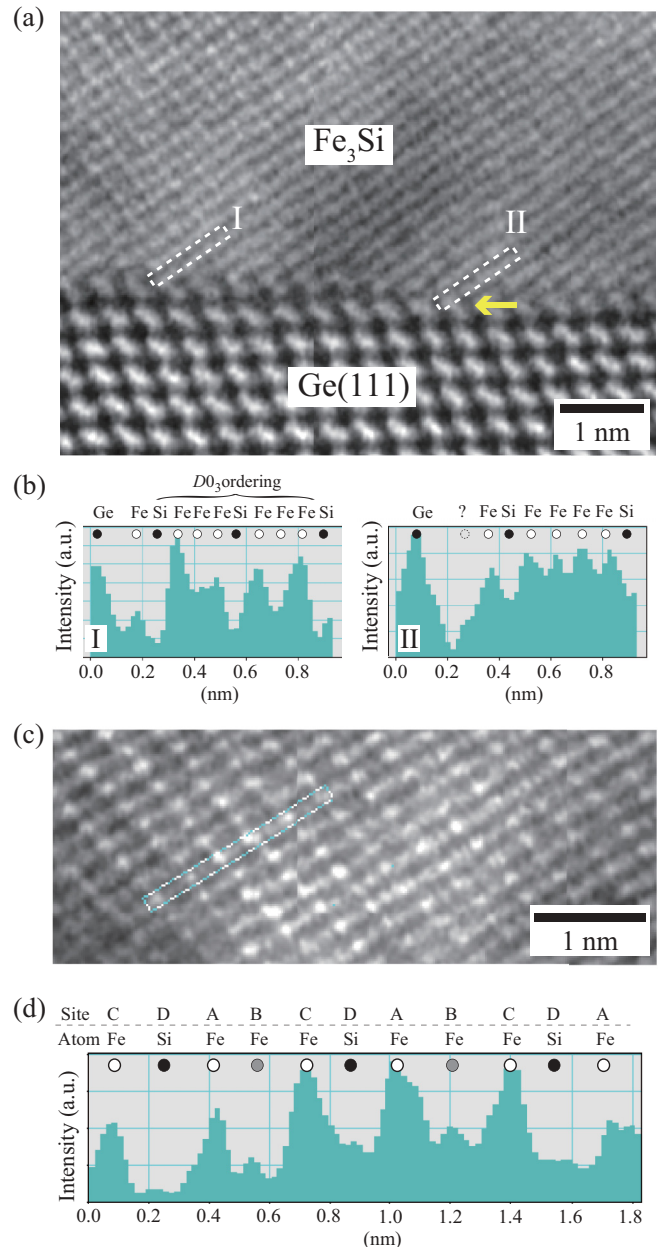

FIG. 1. (Color online) (a) High-resolution cross-sectional TEM image near the Fe_3Si/Ge(111) interface grown at $T_G =$ RT. (b) The intensity profile of the HAADF image from the areas I and II enclosed in Fig. 1(a). (c) HAADF image of the Fe_3Si layer near the interface. The axis of the incident electron beam is parallel to the [1$\bar{1}$0] direction. (d) The intensity profile of the HAADF image from the area enclosed in Fig. 1(c).

occupation in RT-grown Fe_3Si layer with the $D0_3$ ordering. We also note that the intensity of Fe atoms at the B site seems to be weaker than that at the (A,C) sites, indicating relatively many disorders at the B site compared with those at the (A,C) sites. By observing NBD patterns in the Fe_3Si layer, we also obtained $\langle 111 \rangle$ and $\langle 113 \rangle$ superlattice reflections caused by the presence of $D0_3$-ordered structures. The results shown in Fig. 1 are strong evidence for $D0_3$ ordering in Fe_3Si films grown at $T_G =$ RT. By the nanobeam EDS analyses in several points of the Fe_3Si layers, we confirmed that the chemical
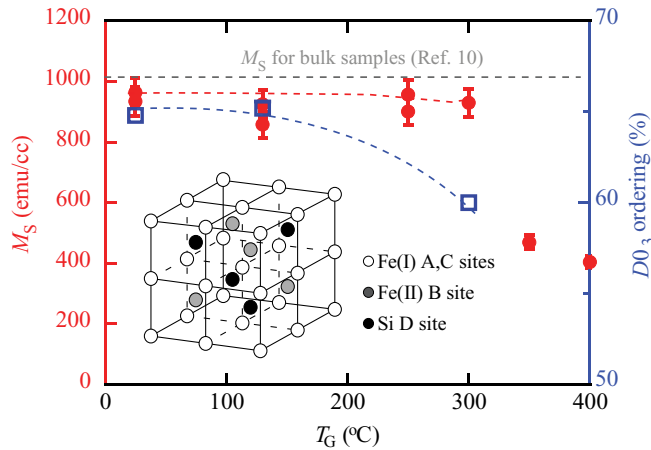
FIG. 2. (Color online) The saturation magnetic moments (M_S) at room temperature (solid circles) and the degree of $D0_3$ ordering (opened squares) of the Fe₃Si(25 nm) films grown at RT $\leqslant T_G \leqslant$ 400 °C. The gray dotted line shows M_S of the bulk sample at 6.5 K in Ref. 10. The inset displays the ideal crystal structure of $D0_3$-type Fe₃Si.

compositional ratio Fe:Si is 75.48:24.52, precisely controlled to 3:1.

To understand the role of T_G, we explored the correlation between magnetic properties and structural ordering for various T_G. Figure 2 shows the saturation magnetic moments (M_S) at room temperature (closed circles) and the degree of the local $D0_3$ ordering (opened squares) for the 25-nm-thick Fe₃Si films as a function of T_G, where M_S was measured directly by using VSM and the degree of the local $D0_3$ ordering was estimated from the combination analyses of the Mössbauer spectra,[27] respectively. In order to estimate M_S, external magnetic fields of ±5 T were applied in the film plane and the background data from the Ge substrate were subtracted from the raw data. First, we focus on M_S versus T_G. Here, the dotted line in this figure shows the M_S value at 6.5 K of the bulk samples formed at 800 °C, reported in Ref. 10. For our Fe₃Si films, M_S values are almost constant for $T_G \leqslant 300$ °C although they are slightly smaller than those for bulk samples. Note that the RT-grown film showed a relatively high Curie temperature more than 600 K (not shown here). Thus, we can achieve high magnetic properties despite the RT growth. For $T_G > 300$ °C, on the other hand, M_S values largely decrease. From the TEM observation of the Fe₃Si/Ge(111) interface formed at $T_G = 300$ °C (not shown here), we found a clear structurally fluctuated region with a thickness of ~3 nm. Previous works with relatively high T_G clearly showed the formation of the other nonmagnetic layers such as germanide compounds caused by the interfacial reaction.[32,33] Thus, we infer that the decrease in M_S for $T_G > 300$ °C is probably due to the formation of the nonmagnetic layers near the interface.

Next, we focus on the degree of the local $D0_3$ ordering of the Fe₃Si films estimated from Mössbauer spectra. For an ideal $D0_3$-ordered Fe₃Si, as illustrated in the inset of Fig. 2, there are two distinct crystallographic and magnetic Fe sites, i.e., Fe(I), occupying the (A,C) sites coordinated with four Fe atoms and four Si atoms, and Fe(II), occupying the (D) site surrounded by eight Fe atoms. If a perfectly $D0_3$-ordered structure is formed,

the areas of Fe(I) and Fe(II) in the ⁵⁷Fe Mössbauer spectra can be divided into 66.6% and 33.3%, respectively. Using the same fitting analyses as Ref. 27, we calculated the existence ratio of the sites attributed to $D0_3$-ordered structures, and then, estimated the degree of $D0_3$ ordering for the Fe₃Si films. The detailed explanation of the analyses will be described in the next section. As in Fig. 2, the degree of $D0_3$ ordering for RT- and 130 °C-grown Fe₃Si films is almost the same and these values are estimated to be ~64.8% and ~65.2%, respectively. However, for 300 °C-grown films, that is reduced down to ~60.0%. As mentioned in the previous paragraph, there were some structural fluctuations at the Fe₃Si/Ge interface. Surely, we observed only $B2$ structures in the Fe₃Si layers just on the fluctuated phases by the NBD patterns of the 300 °C-grown films (not shown here). Also, when we measured chemical composition in this region, we clearly identified the presence of a small amount of Ge. That is, the atomic interdiffusion at the interface occurred due to the high-temperature growth ($T_G \geqslant$ 300 °C). We have also measured ⁵⁷Fe Mössbauer spectra for 400 °C-grown Fe₃Si films. Since the spectra showed significant decrease in magnetic hyperfine fields, the degree of order could not be analyzed by the same method as in Ref. 27.

From these investigations, we revealed that it is not necessary for forming the highly ordered $D0_3$ structure to raise T_G in our MBE system. Even after the post annealing at 300 °C, we could not obtain an improvement of the $D0_3$ ordering.[27] On the other hand, because of the thermal stability for the as-grown samples, it seems important for $D0_3$ ordering to achieve the precise control of the chemical composition. The detailed discussion will be shown in Sec. V. The slightly small M_S for our Fe₃Si films compared with the bulk M_S in Ref. 10 was inferred by the disorder associated with Fe(I), i.e., (A,C) sites, in previous works.[27,34] However, the HAADF observation in Fig. 1 indicated the presence of the disorder associated with Fe(II), i.e., B site. The detailed contents of the disorder in the films will be discussed in the following sections.

IV. THICKNESS DEPENDENCE OF $D0_3$ ORDERING

We examine the effect of thickness on the degree of the $D0_3$ ordering for RT-grown Fe₃Si films. Figure 3(a) shows the ⁵⁷Fe Mössbauer spectra of a 10-nm-thick Fe₃Si film grown at T_G = RT. An evident sextet pattern, typical for magnetically ordered systems, is obtained. Whereas the shapes of the spectra for the 25-nm-thick and 50-nm-thick Fe₃Si films (not shown here) were quite similar to that for the epitaxial Fe₃Si films on MgO reported by Krumme *et al.*,[30] the feature for the 10-nm-thick Fe₃Si film seems to be slightly different. In Fig. 3(a), the spectrum was fitted with seven magnetic environments including Fe(I) and Fe(II) sites in the ideal $D0_3$-ordered Fe₃Si.[8] As described in our previous work,[27] the site number n from 1 to 7 was defined as follows. First, the sites 1 and 2 with the hyperfine magnetic field of 19.4 and 30.4 T are Fe(I) and Fe(II), with four and eight nearest-neighbor Fe atoms, respectively. Note that the site with seven neighboring Fe atoms can not be distinguished from the site 2. Next, the site 3 with 32.8 T represents the Fe atoms in an $A2$-type Fe phase with eight nearest-neighbor Fe atoms. Also, the sites 4, 5, and 6 with 27.4, 23.9, and 13.8 T are the (A,C) or (B,D) sites with six, five, and three nearest-neighbor Fe atoms, respectively.
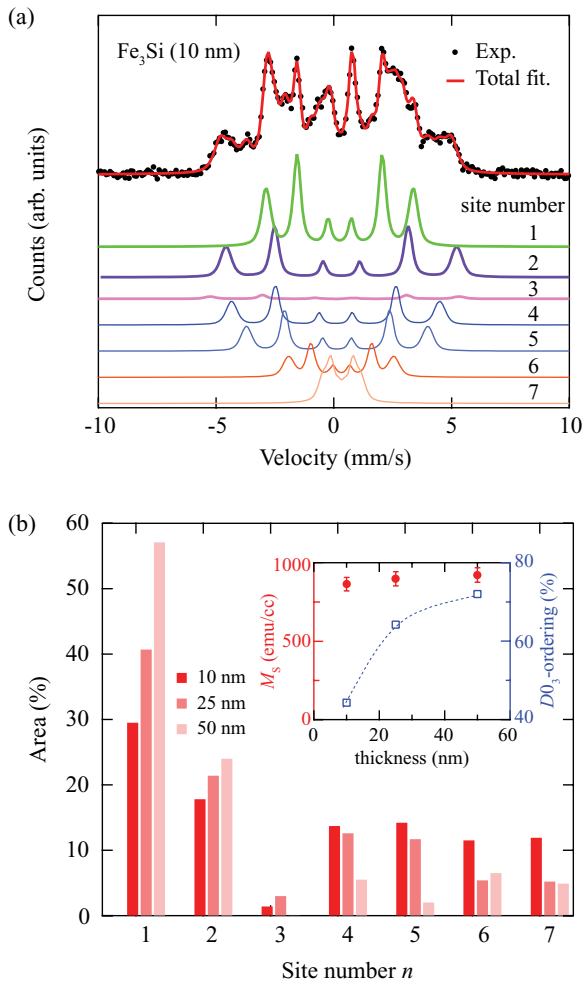
(a)

(b)

FIG. 3. (Color online) (a) Room-temperature ^{57}Fe Mössbauer spectrum (solid circles) of 10-nm-thick Fe$_3$Si films grown at T_G = RT, together with seven fitting curves as denoted in the text. (b) Fitted area versus site number for Fe$_3$Si films with various thicknesses, estimated by CEMS measurements and best fitting. The sites 1 and 2 correspond to Fe(I) and Fe(II), shown in the inset of Fig. 2, for the ideal $D0_3$-ordered Fe$_3$Si. The inset shows the estimated $D0_3$ ordering (%) as a function of film thickness (opened squares), together with M_S at room temperature (solid circles).

Finally, the site 7 with a small hyperfine magnetic field of less than 5 T is regarded as the site which has less than three neighboring Fe atoms. After the fitting of the experimental data with these seven sites, we can evaluate local magnetic environments of the Fe atoms in the 10-nm-thick Fe$_3$Si films. Note that the quadrupole shift was fixed to zero since it is reported to be negligible in bulk Fe$_3$Si.[8] The peak separations after the analyses are also shown in Fig. 3(a).

In Fig. 3(b), we present the percentage of the fitted area versus site number for the room-temperature-grown Fe$_3$Si film with a thickness of 10 nm, together with those of 25 and 50 nm. If a perfectly $D0_3$-ordered Fe$_3$Si film is formed, we should obtain 66.6% for the site 1 and 33.3% for the site 2.[8,17,30] Considering the site occupations, we estimated the local degree of the $D0_3$ ordering for all the films.[27] The inset shows the estimated $D0_3$ ordering (%) as a function of film thickness (opened squares), together with M_S at room temperature

(solid circles). With increasing film thickness, the $D0_3$ ordering is enhanced up to 72.0%. We note that there is a $D0_3$ ordering of 44.3% even for the 10-nm-thick Fe$_3$Si films grown at T_G = RT. The hyperfine magnetic field and isomer shift relative to α-Fe of Fe(I) and Fe(II) are estimated to be 19.4 T and 0.25 mm/s and 30.4 T and 0.08 mm/s, respectively. These values are consistent with those reported in literature.[8,17,30] In our previous work,[27] we have already identified that excess Fe atoms occupying the D site enhance the percentage of the site 3. However, as in Fig. 3(b), the site 3 is less than 3.0% of all the detected magnetic environments around the Fe sites, irrespective of the film thickness. Thus, there is almost no Fe-rich off stoichiometry for these films, which is consistent with almost no marked difference in M_S with increasing thickness in the inset of Fig. 3(b) (solid circles).

On the other hand, we find that the occupation of the sites 4 and 5 for 10-nm-thick and 25-nm-thick Fe$_3$Si films is higher than that for a 50-nm-thick one. In our previous work,[27] we speculated that the increase in the sites 4 and 5 is derived mainly from the site occupation of Si atoms in the (A,C) sites,[27] leading to the disorder associated with the (A,C) sites. However, the increase in the sites 4 and 5 can also be understood by the (B,D) site disorder because of the presence of six, five, and three nearest-neighbor Fe atoms. Actually, in Fig. 1 we observed the presence of the disorder associated with the B site. Furthermore, the 10-nm-thick Fe$_3$Si film has relatively large occupation of Fe atoms in the sites 6 and 7, indicating the three nearest-neighbor and less than three neighboring Fe atoms, respectively. Since such special cases can not be inferred in the bulk region of the $D0_3$-ordered Fe$_3$Si, we now speculate that some disorder with sites 6 and 7 can be promoted near the Fe$_3$Si/Ge interfaces. Surely, unknown structures were observed by HAADF techniques near the Fe$_3$Si/Ge interfaces. Even if we obtain the ideal $D0_3$-ordered Fe$_3$Si films, the Fe atoms connecting with Ge at the interface may show the spectra other than sites 1 and 2. Further detailed study of the $D0_3$ ordering by the Mössbauer spectroscopy measurements should be required for the analyses near the Fe$_3$Si/Ge interfaces.

It should be noted that 44.3% $D0_3$-ordered structures can be obtained even within the 10-nm-thick Fe$_3$Si films, indicating that the $D0_3$ ordering tends to start at the early stage of the growth of the Fe$_3$Si film on Ge(111) even at T_G = RT. Also, the $D0_3$ ordering can be improved by increasing film thickness without a rise of T_G. This also means that there mainly exist disordered structures near the Fe$_3$Si/Ge interfaces, consistent with the HAADF images in Fig. 1. In the next section, we will discuss the possibilities of the presence of the interfacial disorder and of the bulklike thermal stability in RT-grown Fe$_3$Si films based on molecular dynamics simulations.

V. DISCUSSION

A. Interfacial disorder

First, we study the stability of the interface between Fe$_3$Si and Ge by using first-principles molecular dynamics simulations.[35,36] The calculations are based on the density functional theory (DFT) in the generalized gradient approximation (GGA) using the projector-augmented-wave (PAW)
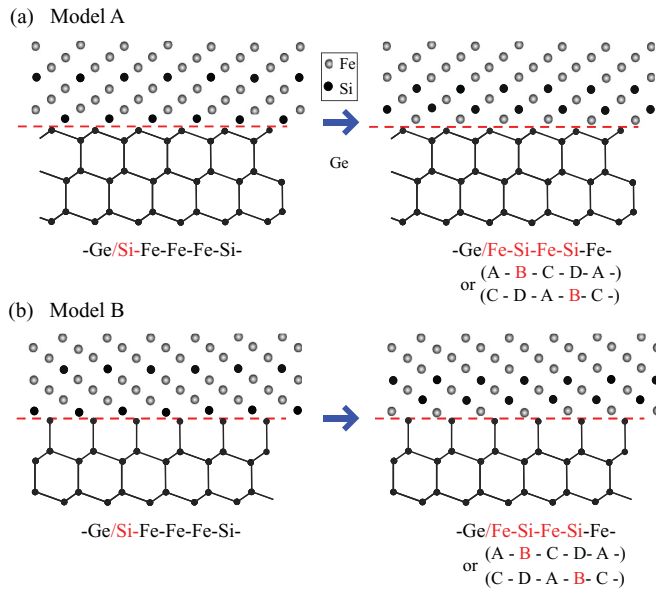
(a) Model A

-Ge/Si-Fe-Fe-Fe-Si-

-Ge/Fe-Si-Fe-Si-Fe-
(A - B - C - D - A -)
or (C - D - A - B- C -)

(b) Model B

-Ge/Si-Fe-Fe-Fe-Si-

-Ge/Fe-Si-Fe-Si-Fe-
(A - B - C - D - A -)
or (C - D - A - B- C -)

FIG. 4. (Color online) Schematic diagrams of atomic arrangements of $Fe_3Si(111)/Ge(111)$ interface for (a) model A and (b) model B. Dashed lines denote interfaces between Fe_3Si and Ge. Left and right show initial and final atomic arrangements before and after molecular dynamics calculations, respectively, for the case of . . .-Ge/Si-Fe-Fe-Fe-. . . stacking in models A and B.

method as implemented in the Vienna *ab initio* simulation package (VASP).[37] We performed molecular dynamics simulations for supercells of Ge (2 ML, bottom)/Ge (3 ML)/Fe_3Si (8 ML)/ vacuum which consists of 20 Ge atoms, 24 Fe atoms, and 8 Si atoms. During the calculations, we fixed the positions of Ge atoms in 2 ML at the bottom of the cells. Here, we assumed atomically abrupt interface between $D0_3$-ordered $Fe_3Si(111)$ and Ge(111), and considered two types of interfacial bonding arrangements, as shown in the left of Fig. 4. The assumed interfacial bonding arrangements are defined as models A and B. Such difference can be induced by the atomic steps observed by the TEM observations [Fig. 1(a)]. Considering these two interfacial bonding arrangements, we conducted molecular dynamics calculations at 300 and 500 K for the following four stacking sequences: -Ge/Si-Fe-Fe-Fe-, -Ge/Fe-Si-Fe-Fe-, -Ge/Fe-Fe-Si-Fe-, and -Ge/Fe-Fe-Fe-Si-. Two of the results, for the case of -Ge/Si-Fe-Fe-Fe-, are shown in the right of Figs. 4(a) and 4(b) for models A and B, respectively. As a result, the stacking sequences can be changed to -Ge/Fe-Si-Fe-Si-Fe-, indicating the site occupation of each atom with -Ge-C-D-A-B-C- in Fe_3Si. Namely, we can see the replacement of the interfacial Si atom with the nearest-neighbor Fe atom. In this calculation, the disorder structures associated with the B site can also be confirmed near the interface, giving rise to the deterioration of the $D0_3$ ordering.

For the other three initial structures, i.e., -Ge/Fe-Si-Fe-Fe-, -Ge/Fe-Fe-Si-Fe-, and -Ge/Fe-Fe-Fe-Si-, we can see no atomic replacements because of the absence of the interfacial Si atom connecting with Ge. Note that for model B, the stacking sequence consisting of Fe and Si layers at the (111) plane was maintained after the calculations. In contrast, for the cases of -Ge/Fe-Fe-Si-Fe- and -Ge/Fe-Fe-Fe-Si- in model A,

the stacking structures were broken (not shown here). These features clearly depended on the atomic intermixing between Fe_3Si and Ge at 500 K. A similar intermixing has already been observed in our MBE conditions ($T_G \geqslant 300$ °C), as described in Fig. 2, and we have seen that post-growth annealing more than 350 °C also induces the atomic intermixing at the interface.[32,38] From these considerations, we can infer that the stacking sequence of -Ge/Fe-Si-Fe-Fe- is more stable. It seems that we can partly observe such atomic rows -Ge/Fe-Si-Fe-Fe-, as shown in Fig. 1(b), despite the presence of many disordered structures near the interface.

In practical MBE conditions, we should consider all of the cases shown above during the growth of Fe_3Si films on Ge(111). In particular, the structural changes and atomic replacements discussed so for can occur at the interface for the growth at finite T_G. Since there are different interfacial atomic arrangements between Fe_3Si and Ge, the structural ordering near the interface can be complicated at the initial stage of the growth. Even for T_G = RT, the interfacial disorder may be induced by the above complicated situations in our MBE conditions. It seems that the presence of the interfacial disordered structures are quite reasonable to explain the structural ordering in the Fe_3Si films. Comparing these calculated results with experimental ones, we can understand that the main structural disorder is derived from the B site in the Fe_3Si film near the interface.

B. Thermal stability

In the previous experimental sections, we have described that rising T_G and post-growth annealing are not required for the formation of the $D0_3$-ordered structures in Fe_3Si films in our MBE conditions. Thus, we hereafter consider the thermal stability of the ordered Fe_3Si.[35,36] The calculations are also based on DFT in GGA using PAW method as implemented in the Vienna *ab initio* simulation package.[37] A superlattice having 12 Fe atoms and 4 Si atoms per unit cell was used for the calculation. Although the study of the site occupation supports the nearly stoichiometric atomic composition in the films, our RT-grown Fe_3Si films have imperfect $D0_3$ ordering from 44.3% to 72.0%, indicating the existence of some microscopic disorder in the films. In order to take into account the influence of the microscopic chemical composition, the next two initial structures are considered, i.e., $D0_3$-ordered structure ($D0_3$) and Fe + B2 structures (Fe + B2), as shown in Fig. 5, where gray and black balls are Fe atoms and Si atoms [$D0_3$ = 4(Fe_3Si), Fe + B2 = 8(Fe) + 4(FeSi)] and the lattice

(a) $D0_3$ (b) Fe+B2

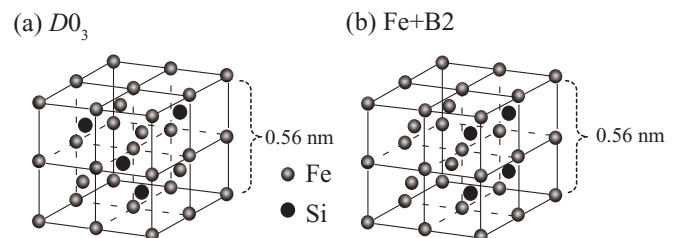~0.56 nm

- Fe
- Si

~0.56 nm

FIG. 5. Schematic diagrams of the initial crystal structure of (a) $D0_3$ and (b) Fe + B2 for the first-principles molecular dynamics calculation.

constant a is assumed to be 0.56 nm. As a result, the critical temperatures t_c (K) of $\sim$2500 K and $\sim$2200 K for $D0_3$ and Fe + $B2$, respectively, were obtained, where t_c is the highest temperature at which each structure can be stable. That is, both $D0_3$ and Fe + $B2$ with $a = 0.56$ nm are markedly stable once the 12 Fe and 4 Si atoms crystallize into $D0_3$ or Fe + $B2$. In other words, even if there is some microscopic disorder in Fe$_3$Si with stoichiometric composition, the structural changes from $D0_3$ or Fe + $B2$ to other structures by annealing hardly occur. As in Fig. 2, high T_G was not so effective to obtain high $D0_3$ ordering. Also, the stoichiometric Fe$_3$Si films with the $D0_3$ ordering of 67.0% could not be improved by the post annealing at $\sim$600 K (350 °C) in our previous work.[27] These experimental features can be explained by the marked thermal stability shown in the above calculation.

On the basis of the above calculations, we discuss low-temperature crystal growth of $D0_3$-ordered Fe$_3$Si. First, we have found that our MBE conditions can achieve $D0_3$-ordered Fe$_3$Si even at room temperature. Second, Fig. 2 clearly indicated that high-growth temperature is not required for the $D0_3$ ordering. Third, in our previous study,[27] the structural ordering of the epitaxial Fe$_{3+x}$Si$_{1-x}$/Ge was strongly affected by their chemical compositions, and an improvement of its structural ordering could not be seen by the post-growth annealing at around 600 K. Considering these facts, we can infer that the obtained $D0_3$-ordered Fe$_3$Si films on Ge(111) at RT are relatively stable. Although both $D0_3$ and Fe + $B2$ can be formed because of the thermal stability, our actual MBE can only realize more than 70% of the local degree of $D0_3$ for 50-nm-thick films at RT. If our MBE conditions give local Fe-rich or Fe-poor structures during the growth, Fe + $B2$ structures shown in Fig. 5(b) should easily be formed. Hence, we can consider that our MBE growth has one of the special growth conditions to obtain $D0_3$-ordered Fe$_3$Si, induced by the local stoichiometry of the supplied Fe and Si atoms on top of the Ge(111) surface.

Previously, Yoshitake *et al.* also reported RT epitaxial growth of Fe$_3$Si films on Si(111) by using facing target dc sputtering.[23] The epitaxial growth on the Si(111) plane can be explained by the same mechanism of our growth process in the Fe$_3$Si films.[25–27] However, there is a critical difference in the structural ordering between their work[23] and ours (this work). Although they have obtained $B2$-ordered Fe$_3$Si films at RT, they could not obtain $D0_3$-ordered structures.[39] As described in Fig. 5(b), if they have local inhomogeneity of the chemical composition in the crystal growth process, Fe + $B2$ having a marked stability can easily be formed. Therefore, the difference in the structural ordering between their work[23] and this work can be understood by the difference in the local stoichiometry of the supplied Fe and Si atoms in the crystal growth process. Although the MBE process with Knudsen cells can realize the homogeneous supply of Fe and Si atoms with an accurate control of cell temperature, the sputtering process with a plasma-enhanced technique and an Fe$_{3+x}$Si$_{1-x}$-alloy target probably causes inhomogeneous supply of Fe and Si atoms on the surface of the substrate, leading mainly to the formation of the Fe + $B2$ structure at RT. Considering the difference in the local stoichiometry of the supplied Fe and Si atoms among the crystal growth techniques, we speculate that the MBE techniques for epitaxial Fe$_3$Si films on GaAs(100) (Refs. 20, 21, and 31) can also achieve the RT $D0_3$ ordering. On the contrary, the sputtering and pulsed-laser deposition can not achieve it because of the lack of the local stoichiometry of the supplied Fe and Si atoms on the surface of the substrate. In our opinion, if one can demonstrate the local stoichiometry of the supplied atoms such as Co, Fe, Si, Mn, and Al, half-metallic Heusler compounds with $L2_1$-ordered structures[2,4,5] may be formed at RT for high-performance spintronic devices.

VI. CONCLUSION

By using a molecular beam epitaxy (MBE) technique, $D0_3$-ordered Fe$_3$Si films were successfully grown even at room temperature. Since the interfacial reactions between Fe$_3$Si and Ge were induced, the higher growth temperatures were not effective to obtain the highly ordered $D0_3$ structures. Interestingly, even for the room-temperature growth, the degree of the $D0_3$ ordering was improved from 44.3% to 72.0% with increasing film thickness from 10 to 50 nm. We concluded that the $D0_3$ ordering occurs at the early stage of the growth process and high-temperature heat treatments do not necessarily result in the formation of $D0_3$-ordered Fe$_3$Si, which is consistent with our previous work on the post-growth annealing. Considering the experimental data and the calculated results, we can understand that the main structural disorder is derived from the B site in the Fe$_3$Si film near the interface. We inferred that the room-temperature $D0_3$ ordering arises from the local stoichiometry of the supplied atoms in MBE conditions.

*hamaya@ed.kyushu-u.ac.jp
[1]R. A. de Groot, F. M. Mueller, P. G. van Engen, and K. H. J. Buschow, Phys. Rev. Lett. **50**, 2024 (1983).
[2]I. Galanakis, P. H. Dederichs, and N. Papanikolaou, Phys. Rev. B **66**, 174429 (2002).
[3]M. Yamamoto, T. Marukame, T. Ishikawa, K. Matsuda, T. Uemura, and M. Arita, J. Phys. D: Appl. Phys. **39**, 824 (2006).
[4]G. H. Fecher and C. Felser, J. Phys. D: Appl. Phys. **40**, 1582 (2007).
[5]K. Inomata, N. Ikeda, N. Tezuka, R. Goto, S. Sugimoto, M. Wojcik, and E. Jedryka, Sci. Technol. Adv. Mater. **9**, 014101 (2008).

[6]T. Kimura, N. Hashimoto, S. Yamada, M. Miyao, and K. Hamaya, NPG Asia Materials **4**, e9 (2012).

[7]K. Hamaya, N. Hashimoto, S. Oki, S. Yamada, M. Miyao, and T. Kimura, Phys. Rev. B **85**, 100404(R) (2012).

[8]M. B. Stearns, Phys. Rev. **129**, 1136 (1963).

[9]M. B. Stearns, Phys. Rev. B **4**, 4069 (1971).

[10]W. A. Hines, A. H. Menotti, J. I. Budnick, T. J. Burch, T. Litenta, V. Niculescu, and K. Raj, Phys. Rev. B **13**, 4060 (1976).

[11]V. Niculescu, J. I. Budnick, W. A. Hines, K. Raj, S. Pickart, and S. Skalski, Phys. Rev. B **19**, 452 (1979); V. A. Niculescu, T. J. Burch, and J. I. Budnick, J. Magn. Magn. Mater. **39**, 223 (1983).

[12]S. Fujii, S. Ishida, and S. Asano, J. Phys. Soc. Jpn. **64**, 185 (1995).

[13]J. Kudrnovský, N. E. Christensen, and O. K. Andersen, Phys. Rev. B **43**, 5924 (1991).

[14]E. G. Moroni, W. Wolf, J. Hafner, and R. Podloucky, Phys. Rev. B **59**, 12860 (1999).

[15]A. Bansil, S. Kaprzyk, P. E. Mijnarends, and J. Tobola, Phys. Rev. B **60**, 13396 (1999).

[16]N. I. Kulikov, D. Fristot, J. Hugel, and A. V. Postnikov, Phys. Rev. B **66**, 014206 (2002).

[17]M. Miyazaki, M. Ichikawa, T. Komatsu, and K. Matusita, J. Appl. Phys. **71**, 2368 (1992).

[18]F. Lin, D. Jiang, X. Ma, and W. Shi, Thin Solid Films **515**, 5353 (2007).

[19]Kh. Zakeri, I. Barsukov, N. K. Utochkina, F. M. Römer, J. Lindner, R. Meckenstock, U. von Hörsten, H. Wende, W. Keune, M. Farle, S. S. Kalarickel, K. Lenz, and Z. Frait, Phys. Rev. B **76**, 214421 (2007).

[20]J. Herfort, H.-P. Schönherr, and K. H. Ploog, Appl. Phys. Lett. **83**, 3912 (2003).

[21]J. Herfort, H.-P. Schönherr, K.-J. Friedland, and K. H. Ploog, J. Vac. Sci. Technol. B **22**, 2073 (2004).

[22]A. Ionescu, C. A. F. Vaz, T. Trypiniotis, C. M. Gürtler, H. García-Miquel, J. A. C. Bland, M. E. Vickers, R. M. Dalgliesh, S. Langridge, Y. Bugoslavsky, Y. Miyoshi, L. F. Cohen, and K. R. A. Ziebeck, Phys. Rev. B **71**, 094401 (2005).

[23]T. Yoshitake, D. Nakagauchi, T. Ogawa, M. Itakura, N. Kuwano, Y. Tomokiyo, T. Kajiwara, and K. Nagayama, Appl. Phys. Lett. **86**, 262505 (2005).

[24]K. Kobayashi, T. Sunohara, M. Umada, H. Yanagihara, E. Kita, and T. Suemasu, Thin Solid Films **508**, 78 (2006).

[25]K. Hamaya, K. Ueda, K. Kasahara, Y. Ando, T. Sadoh, and M. Miyao, Appl. Phys. Lett. **93**, 132117 (2008).

[26]T. Sadoh, M. Kumano, R. Kizuka, K. Ueda, A. Kenjo, and M. Miyao, Appl. Phys. Lett. **89**, 182511 (2006); K. Hamaya, H. Itoh, O. Nakatsuka, K. Ueda, K. Yamamoto, M. Itakura, T. Taniyama, T. Ono, and M. Miyao, Phys. Rev. Lett. **102**, 137204 (2009); M. Miyao, K. Hamaya, T. Sadoh, H. Itoh, and Y. Maeda, Thin Solid Films **518**, S273 (2010).

[27]K. Hamaya, T. Murakami, S. Yamada, K. Mibu, and M. Miyao, Phys. Rev. B **83**, 144411 (2011).

[28]Y. Ando, K. Hamaya, K. Kasahara, Y. Kishi, K. Ueda, K. Sawano, T. Sadoh, and M. Miyao, Appl. Phys. Lett. **94**, 182105 (2009); Y. Ando, K. Kasahara, K. Yamane, K. Hamaya, K. Sawano, T. Kimura, and M. Miyao, Appl. Phys. Express **3**, 093001 (2010); K. Hamaya, Y. Ando, T. Sadoh, and M. Miyao, Jpn. J. Appl. Phys. **50**, 010101 (2011).

[29]K. Kasahara, Y. Baba, K. Yamane, Y. Ando, S. Yamada, Y. Hoshi, K. Sawano, M. Miyao, and K. Hamaya, J. Appl. Phys. **111**, 07C503 (2012).

[30]B. Krumme, C. Weis, H. C. Herper, F. Stromberg, C. Antoniak, A. Warland, E. Schuster, P. Srivastava, M. Walterfang, K. Fauth, J. Minár, H. Ebert, P. Entel, W. Keune, and H. Wende, Phys. Rev. B **80**, 144403 (2009).

[31]S. I. Makarov, B. Krumme, F. Stromberg, C. Weis, W. Keune, and H. Wende, Appl. Phys. Lett. **99**, 141910 (2011).

[32]Y. Maeda, T. Jonishi, K. Narumi, Y. Ando, K. Ueda, M. Kumano, T. Sadoh, and M. Miyao, Appl. Phys. Lett. **91**, 171910 (2007).

[33]R. Jaafar, D. Berling, D. Sébilleau, and G. Garreau, Phys. Rev. B **81**, 155423 (2010).

[34]B. Jenichen, V. M. Kaganer, J. Herfort, D. K. Satapathy, H. P. Schönherr, W. Braun, and K. H. Ploog, Phys. Rev. B **72**, 075329 (2005).

[35]S. Dennler and J. Hafner, Phys. Rev. B **73**, 174303 (2006).

[36]J. Hafner and D. Spisák, Phys. Rev. B **75**, 195411 (2007).

[37]G. Kresse and J. Furthmuller, Comp. Mater. Sci. **6**, 15 (1996).

[38]Y. Ando, K. Hamaya, K. Kasahara, K. Ueda, Y. Nozaki, T. Sadoh, Y. Maeda, K. Matsuyama, and M. Miyao, J. Appl. Phys. **105**, 07B102 (2009).

[39]Even for the growth on Si(111), we have already obtained $D0_3$-ordered Fe_3Si films at RT and the degree of $D0_3$ ordering is roughly estimated to be $\sim 52\%$. Thus, the difference in the used substrate between Si and Ge is not a critical problem for the structural ordering of the Fe_3Si films at room temperature.